

Point Adversarial Self Mining: A Simple Method for Facial Expression Recognition in the Wild

Ping Liu, Yuewei Lin, Zibo Meng, Weihong Deng, Joey Tianyi Zhou, and Yi Yang

Abstract—In this paper, the Point Adversarial Self Mining (PASM) approach, a simple yet effective way to progressively mine knowledge from training samples, is proposed to produce training data for CNNs to improve the performance and network generality in Facial Expression Recognition (FER). In order to achieve a high prediction accuracy under real-world scenarios, most of the existing works choose to manipulate the network architectures and design sophisticated loss terms. Although demonstrated to be effective in real scenarios, those aforementioned methods require extra efforts in network design. Inspired by random erasing and adversarial erasing, we propose PASM for data augmentation, simulating the data distribution in the wild. Specifically, given a sample and a pre-trained network, our proposed approach locates the informative region in the sample generated by point adversarial attack policy. The informative region is highly structured and sparse. Comparing to the regions produced by random erasing which selects the region in a purely random way and adversarial erasing which operates by attention maps, the located informative regions obtained by PASM are more adaptive and better aligned with the previous findings: not all but only a few facial regions contribute to the accurate prediction. Then, the located informative regions are masked out from the original samples to generate augmented images, which would force the network to explore additional information from other less informative regions. The augmented images are used to finetune the network to enhance its generality. In the refinement process, we take advantage of knowledge distillation, utilizing the pre-trained network to provide guidance and retain knowledge from old samples to train a new network with the same structural configuration. Comparing to previous works using complex architectures, our method can achieve high performance with a standard structure of moderate size, *e.g.*, ResNet-34, by self-mining related knowledge from the given input. Although our method is apparently simple, it achieves high prediction accuracy on two widely used in-the-wild datasets for facial expression recognition. Notably, our method achieves 88.68 on RAF-DB and 73.59 on FER2013, outperforming previous works under the same settings.

Index Terms—Facial Expression Recognition, In-the-wild Data, Point Adversarial Attack.

1 INTRODUCTION

Facial activity analysis aims to comprehend the underlying human emotions and establish efficient communications between humans and humans or humans and computers. Due to its emerging applications in human-computer interaction, facial activity recognition has received massive interest among the research community. In the past decade, with the rapid development of modern Convolutional Neural Networks(CNNs), the FER accuracy has been boosted significantly.

As a “data-hungry” method, CNNs require huge amount of data with annotations of high quality to train. However, due to privacy concerns and expensive labor cost, collecting and annotating massive data for facial expression recognition (FER) has never been an easy task. Existing datasets for facial expression recognition can be categorized into two cases: lab-controlled datasets and in-the-wild datasets. In lab-controlled datasets, such as CK+ [1], the collecting environment is highly controlled, *e.g.*, frontal exaggerated expressive faces with limited occlusions and minimal illumination changes. These lab-controlled datasets have been

widely adopted for developing and evaluating facial expression recognition systems [2], [3], [4], [5], [6], [7], [8], [9], [10], [11]. However, the lab-controlled datasets cannot reflect the facial expression under real circumstances which makes the systems developed using those databases hard to generalize well in real applications. To include more variations, several in-the-wild datasets have been created most recently. Compared with those from the lab-controlled datasets, samples from the in-the-wild datasets are more challenging, where spontaneous head poses and ornaments on those samples bring about various occlusions, and therefore make the extracted features suffer from serious interference.

In order to improve the FER accuracy when handling non lab-controlled data, various methods have been proposed to enhance the generality of CNNs, which can be roughly categorized into two subsets: attention mechanism based and auxiliary data based methods. [14], [15], [16] propose to utilize attention mechanism to simulate the human perception system for processing in-the-wild data. The attention map, can be generated either by following the weakly supervised object localization strategy [14], or by the confidence score provided by an occlusion/landmark detector [15]. For example, [14] designs a weakly supervised local-global relation network to generate attention maps, indicating the facial regions crucial to the prediction. [15] detects face landmarks, and utilizes the landmark confidence scores as the corresponding occlusion level. Based on the confidence score, the network can explicitly place appropriate focus on different facial regions to make an

• *P. Liu, Joey Zhou are with Institute of High Performance Computing, Agency for Science, Technology, and Research, Singapore.*
 • *Y. Yang are with Centre for Artificial Intelligence, University of Technology Sydney, Sydney, Australia.*
 • *W. Deng is with Pattern Recognition and Intelligent System Laboratory, Beijing University of Posts and Telecommunications, Beijing, China.*
 • *Y. Lin is with Brookhaven National Laboratory, Upton, NY, USA.*
 • *Z. Meng is with InnoPeak Technology Inc., Palo Alto, CA, USA.*

Manuscript received April 19, 2005; revised August 26, 2015.

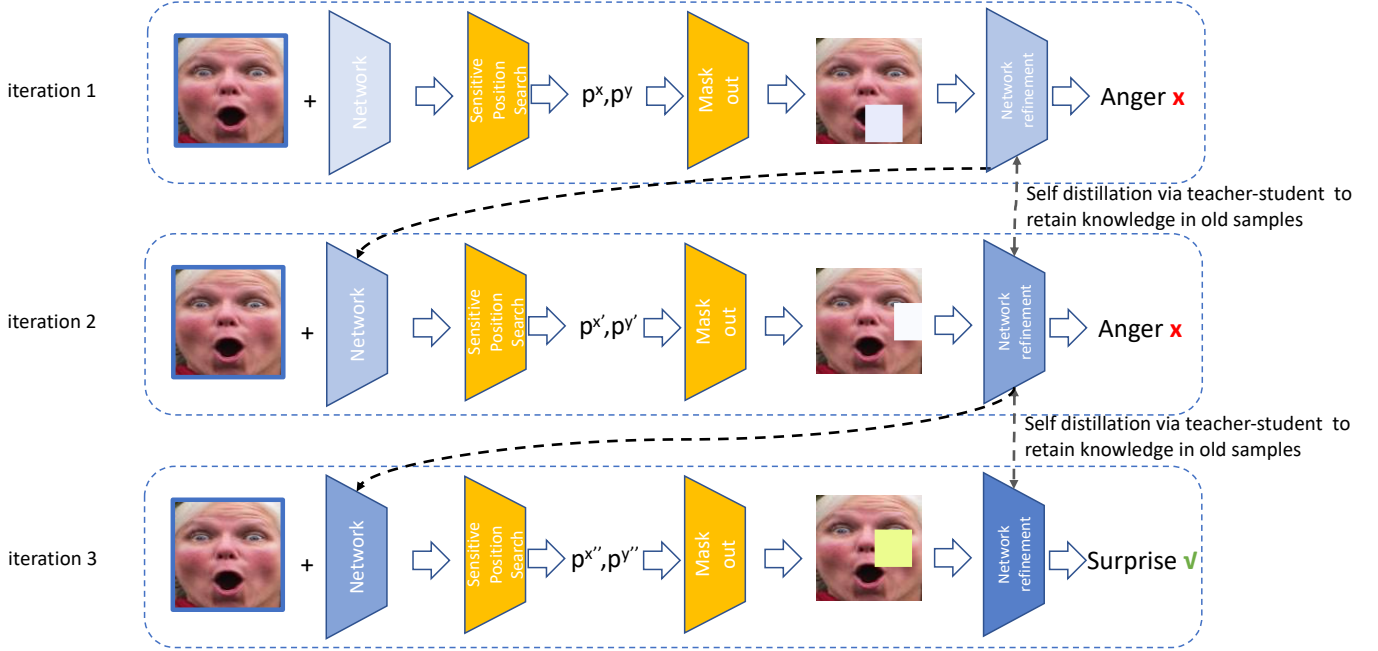


Fig. 1: The pipeline of the proposed PASM. In the first beginning, PASM utilizes the given samples to train a network with a moderate size for facial expression recognition. After training the network, we analyze the model-specified contribution for different regions to the classification in each sample, and locate the most sensitive position in the sample via a point adversarial attack method [12]. Then we mask out the patch centered at the located position and treat the erased version as an augmented case. Those augmented cases are utilized to refine the network, aiming to boost the network performance in facial expression recognition in the wild. Specifically, the trained network in the first beginning is utilized as a teacher network to provide guidance in the network refinement process by following the strategy of knowledge distillation [13]. After finishing the refinement in the first iteration, we have a network with better generalities. In the second and third iteration, we utilize the updated network and the original data to repeat the processes (sensitive positions search, mask out local regions, and refine the network) again, aiming to improve the generality of the network further without complicating the network structure or introducing new loss functions. We iteratively repeat the aforementioned process until a pre-specified iteration number reached or no further improvement is observed. As the iterations go, the generality of the network keeps increasing, and the prediction accuracy becomes higher. Best viewed in color.

accurate prediction. Although the attention-based methods have been well demonstrated for FER, they might need architecture modifications and require additional parameters.

Can we improve FER accuracy by keeping the model relatively simple, *i.e.*, neither using a complex architecture nor modify an existing network heavily? In this paper, we argue that we can focus on the training images rather than the model to achieve the above-mentioned goal, since the useful information beneficial to our target task exists in the original given images after all. However, since the number of the existing annotated samples are limited, it is hard to cover all the variations in real scenarios utilizing those limited data to train a CNN.

To this end, we propose a novel data augmentation strategy working in a self-mining, manner, named Point Adversarial Self Mining (**PASM**). By considering the statistical characteristics of each sample and a trained network, our method is to adaptively locate the most informative regions in each image. Since each sample has its own statistical distribution, the most informative region in each sample located by our method is different from other samples. We then mask out the information around this located position. By doing this, the network is forced to explore additional information from other (less informative in the current time)

regions. The image with salient regions masked out, alongside with the trained network, collaborate as a “teacher” to guide the learning of a new “student” network. The trained student network is demonstrated to have better generality comparing with its teacher. In the whole process, the key information is mined from the images themselves without modifying the network or the loss terms.

In particular, PASM firstly utilizes the training data to train a network with a proper size for facial expression recognition. Note that, since PASM is model-agnostic, any network architectures can be employed, *e.g.*, ResNet [17], VGG [18]. Then we use the trained model to generate a heatmap, which reflects the model-specified contribution of different facial regions, for each training sample, in which, the most important region for FER, *i.e.* with the highest scores, is located via a point adversarial attack method [12]. As demonstrated in [12], point adversarial attack [12] is able to “generate one-pixel adversarial perturbations” to fool the networks. In FER, the located informative position on each sample can tell us which region on the face is the most important and the easiest to mislead the network. To suppress the potential negative impact introduced by the salient region in each sample, we mask out the patch centered at the located position and treat the masked im-

age is used as an augmented sample. Those augmented samples are utilized to finetune the network, aiming to boost the performance in FER in the wild. Specifically, the trained network using the original training samples is utilized as a teacher network to provide guidance in the network finetuning by following the strategy of knowledge distillation [13]. After finishing the finetuning, we have a network with better generalities. We utilize the updated network and the original data to repeat the processes (salient location search, masking out local regions, and finetuning the network) aiming to improve the generality of the network further without complicating the network structure or introducing new loss functions. We can iteratively repeat the aforementioned process until a pre-specified iteration number reached or no further improvement is observed. As the iterations go, the generality of the network keeps increasing, and the prediction accuracy becomes higher. The whole process is illustrated in Figure 1. By adaptive select the informative region and mask out the corresponding information in the given sample, the augmented samples can be closed to the data with different variations, which exist in the real scenarios but are expensive to collect and label.

Our proposed PSAM is inspired and sharing similar motivations with two previous data augmentation methods: random erasing [19] and adversarial erasing [20], where sub-regions were erased from the original “clean” image to produce new samples as augmented data to training a CNN to improve the generality under real-world scenarios. Although the motivation is similar, it should be noted that there are a few significant differences between our method and [19], [20]. [19] chooses the sub-regions to erase in a pure random way, without considering the characteristics of the input and the network. In other words, the erased sub-regions might occur in a region providing few information to the final prediction. On the contrary, our method behaves in a more adaptive way by considering the statistical information of each sample and the network. Comparing to [20] using an attention map to select regions to erase, the erased patch by our method is more structured and sparse, which aligns heavily with a discovery in the face analysis problems: not all facial regions but only a few contribute to the final predictions [10], [21].

To sum up, our main contributions in this work are as follows:

(1) We propose a simple yet effective method, named Point Adversarial Self Mining (PASM), to self-mine knowledge from given samples. The self-mined knowledge is utilized to generate augmented samples, which collaborate with a pre-trained network in a teacher-student manner for improving the network generality.

(2) We propose an iterative and progressive strategy, where, in each iteration, PASM can locate a different informative position in each sample based on the current network status, and iteratively improves the network generality and capability.

(3) We conduct extensive experiments on challenging in-the-wild facial expression datasets collected under real-world settings. Our method, although simple, is better or at least comparable compared with the previous methods utilizing complex architectures or dedicated loss functions.

Our work achieves 87.54% on RAF-DB dataset based on ResNet-34, which is the new state-of-the-art under the same setting. On Occluded-RAF-DB and Pose-RAF-DB, our method outperforms the previous works [22] by approximate 3%.

2 RELATED WORK

In this section, we will elaborate previous works that are most related to our works, including facial expression recognition approaches, data-augmentation strategies, and adversarial attack methods.

2.1 Facial Expression Recognition

Facial expression recognition is an image-level classification research topic, which has been considered as a combination of three major steps: feature learning, feature selection, and classifier construction [10]. Before the dominance of convolutional neural networks in this field, hand-crafted feature-based methods have been exhaustively studied for facial expression recognition. As elaborated by the recent survey papers [23], [24], [25], various hand-crafted features, such as Gabor-wavelet-based features [3], [4], [6], Histograms of Oriented Gradients (HOGs) [7], [8], Local Binary Pattern (LBP) [26], [27], [28], have been developed and well demonstrated for facial activity analysis using data collected under lab-controlled settings. In the past decade, as convolutional neural networks have shown promise in different computer vision tasks, researchers in facial expression recognition start to shift their attention from hand-crafted features to deep features [10], [11], [15], [29], [30], [31]. Comparing to their hand-crafted contemporaries, whose designing heavily depends on human expertise, deep features can be learned in a data-driven manner and have better generality and performance on challenging datasets. To improve the learning capacity of CNNs for facial expression recognition, various architectures have been developed and studied, such as Deep Belief Networks [10], ResNets [11], InceptionNets [29], Generative Adversarial Networks (GANs) [30], [32], [33]. Most recently, researchers found that utilizing information from other modalities, such as audio [34], [35], can help to boost the emotion recognition performance. For a systematic review for deep learning in facial expression recognition, please refer to [36].

2.2 Data Augmentation

Data augmentation is one of the strategies that can effectively prevent deep networks from over-fitting. As the architectures of the deep networks become deeper and more complicated, the number of parameters has increased dramatically. Without enough labeled data, it is easy for those networks to over-fit and lose the generality. In particular, as pointed out in [19], in an extreme case, an over-fitted model might achieve perfect accuracy for the training data while performs poorly on unseen data. To deal with the over-fitting problem in convolutional neural networks, various data augmentation strategies have been proposed and employed [19]. The basic idea of data augmentation is to introduce more variations into the training data without changing the statistical distribution of the original data.

The most common and frequently used data augmentation techniques include random cropping, random flipping, and random color jittering. Random cropping is to crop off sub-patches from a given input; random flipping is to flip the given input in a probability; and random color jittering is to randomly change the values in a pre-defined color space for each given sample. The efficacy of those three data augmentation strategies have been demonstrated in [18], [37]. In the past two years, two novel data augmentation methods, namely mixup [38] and random erasing [19], have been proposed and brought about fresh ideas to data augmentation field. Mixup [38] combines pairs of examples and corresponding labels in a convex manner in order to generate new training samples. Random erasing [19] randomly select a position in a given input and erase the pixels around the selected position. All of those proposed data augmentation methods are complementary and can be combined together to train a deep neural network, which has been experimentally proven to be effective. Interested readers can refer to [39] for a broad understanding of data augmentation in deep learning.

Note that, while random erasing [19] appears similar to our work at the first glance, there are significant differences between them: 1) random erasing [19] select the patch to erase from the given input in a purely random manner, while our method selects the erasing position by considering the underlying model-specified contribution distribution. 2) our method can work in a progressive way and continuously improve the model performance, which [19] fails to achieve. Comparing to [20], the erased part is more structured and sparse, which aligns well with the previous findings in face related problems: only a sparse set of facial regions make the key contributions to the final prediction.

2.3 Adversarial Attack

With the successful application of deep neural networks in various computer vision tasks, CNNs have been deployed in more safety-critical scenarios, such as autonomous driving, financial fraud detection, etc. However, recent works [40] pointed out that deep neural networks are not as stable as we expected. In contrary, they are vulnerable to adversarial examples, which are the samples intentionally designed to mislead a trained deep neural network to make incorrect predictions. To achieve this goal, adversarial examples need to be synthesized based on the model capability and given input [41].

Generally, adversarial attack can be categorized into two groups: white-box attack [42], [43], [44] and black-box attack [12], [45]. The difference between them is the availability of network information, *e.g.*, parameters, gradients, etc. Specifically, in a white-box attack setting, those network information is all available to the attackers; while in black-box attack, it is unavailable to adversaries. Correspondingly, in a white-box attack, the model architecture and parameters are utilized to create the adversarial samples which can attack the model to the most, while in the black-box attack, a feed-and-query strategy is the first choice for adversaries. The most frequently used white-box attack policies include Fast Gradient Sign Method (FGSM) [42], Deep Fool [43], Projected Gradient Descent (PGD) [44], etc. Recently, researchers have conducted a few works toward black-box

attack. [45] proposes to extend natural evolutional strategies to estimate gradient for black-box image attack. [46] studies the feasibility of utilizing the adversarial example transferability for black-box attack on static images. Readers can refer to [41] for a systematic review of the adversarial attack.

3 METHODOLOGY

This section illustrates the details of the proposed PASM for facial expression recognition in the wild. As illustrated in Alg. 1, first, we pre-train a network based on the original training samples; second, given the trained network in the previous step, the most sensitive position for each image is located by considering the statistical characteristics of the given sample produced by the trained network; third, local regions are masked out around the located position to generate an augmented sample, which is fed to the network for finetuning to improve its generalities.

3.1 Network Pre-training

In the first step, we train a network based on the original training samples, *i.e.*, $\{x_i, y_i\}$, where x_i denotes each sample and y_i denotes the corresponding label. The target network is denoted as $F(w)$, where w denotes the model parameters. In order to conduct a fair comparison, we choose ResNet-34 [17] and VGG16 [18] pretrained by ImageNet [47]. We reset the output number of the chosen ResNet-34 and VGG16 to fit to the number of our interested class size for facial expression recognition, *i.e.*, 7. We choose cross-entropy loss to train our target networks, which is formulated as:

$$\min_w \frac{1}{N} \sum_i^N \text{CrossEntropy}((F(w, x_i), y_i)) \quad (1)$$

where N denotes the number of training samples.

3.2 Sensitive Location Search via Point Adversarial Attack

The purpose of this step is to locate the most sensitive position based on the given sample and the pre-trained network obtained in the previous step. In facial activity analysis, previous studies [10], [21] show that not all facial regions make equal contributions in recognizing facial expressions. As a matter of fact, only a small set of facial regions provide effective and useful information to make the right prediction in facial expression recognition, which has been experimentally proven in [10], [21], [28]. Therefore, we need to find an effective mechanism to locate the most sensitive location in an adaptive manner, taking the characteristics of each sample and the status of the current network into consideration.

To solve the aforementioned problem, we utilize point adversarial attack technique [12] for the informative position location in each sample. Point adversarial attack is to select one solo position from the given sample and conduct perturbation to fool the network. Although only one position is found in each given sample, the perturbation conducted at the position can still mislead the network to make an incorrect prediction since the perturbation is

generated by considering each sample characteristics and the current network status.

The general goal of adversary attack can be formulated as follows:

$$\begin{aligned} \max_{e(x)^*} & F(\mathbf{x} + e(\mathbf{x}), w) \\ \text{s.t.} & \|e(\mathbf{x})\|_0 \leq d \end{aligned} \quad (2)$$

where F denotes the target network, \mathbf{x} denotes the original input without perturbations, $e(\mathbf{x})$ is an “additive adversarial perturbation” [12] with respect to \mathbf{x} , $F(\mathbf{x}, w)$ is the prediction for \mathbf{x} while $F(\mathbf{x} + e(\mathbf{x}), w)$ is the prediction for the perturbed input. Adversarial attack aims to find perturbations under a specified constraint to lead the network to make incorrect predictions. In this work, we generate the perturbations under a sparse constraint by setting d as 1, which is aligned with the previous discovery that not all but only a few face regions provide the key information for making predictions.

We follow the same strategy proposed in [12] to locate the informative region, which is generated by the point attack information. The key calculation part is based on differential evolution. Concretely, the perturbation for each given sample is encoded into an array. The encoded array corresponds to a candidate solution. Each candidate solution denotes a fixed number of perturbations, each of which has the perturbation information, *i.e.*, x-y coordinates. The candidate solution evolves in an iterative way. At each iteration, new candidate solutions are produced based on differential evolution, which can be formulated as:

$$x_i(g+1) = x_{r1}(g) + F(x_{r2}(g) - x_{r3}(g)) \quad (3)$$

where x_i is a candidate solution element, $r1, r2, r3$ are random numbers¹, F is a predefined scale factor, g denotes the generation index. As the formulation illustrates, “each candidate solution compete with their corresponding parents based on the index”, and “only the winner” can be used in next iteration.

For each sample from the training set, we use point adversarial attack method discussed above to analyze the statistical information of the sample and the network pre-trained, generate the pixel adversarial information for the given sample, which is denoted as (p^x, p^y) . The generated adversarial information will be used to mask out the corresponding local information for the given sample, generating augmented samples to improve the network generality.

3.3 Generating Augmented Samples for Network Refinement

In this step, we utilize the sensitive positions located in the previous step to generate augmented samples by erasing the local information around the located position. We aim to utilize the generated samples to refine the network and improve the network generality. Since the perturbations added at those located positions are easy to mislead the network, we choose to mask out the information around the located positions for augmented sample generation. Actually, this is the key difference between our work from the random erasing [19]. With a similar goal to improve

1. $r1 \neq r2 \neq r1$

network generalities, [19] masks out a local patch centered at a position *randomly* chosen. On the contrary, our method locates the most sensitive position by considering the characteristics of the given input and corresponding network. Therefore, our method is more adaptive and effective, which is demonstrated in the experimental results.

Concretely, for each given sample x_i , assume its size is $W \times H$, where W denotes the sample width and H denotes the sample height, the sensitive position located in Sec. 3.2 is p^x, p^y , the patch size for masking is denoted as S . Then in each sample x_i , we select a patch region with the size of $S \times S$ located at position p_i^x, p_i^y , and mask out the local region to generate an augmented sample. The generated samples will be used to refine the network, aiming to improve its generality.

Algorithm 1: Point Adversarial Self Mining

Input: Input image set $\{\mathbf{x}_i, y_i\}$, $1 \leq i \leq N$; Image sizes W_i and H_i ; Patch size S , Iteration number $iter$

Output: Network parameter w^*

- 1 training target network with input images $\{\mathbf{x}_i, y_i\}$, get an initialization for w ;
- 2 **for** $ind = 1, \dots, iter$ **do**
- 3 **for** $i = 1, \dots, N$ **do**
- 4 sample an image $\{\mathbf{x}_i, y_i\}$ from the given set;
- 5 for the sampled $\{\mathbf{x}_i, y_i\}$, utilize Equ. 3 to generate the sensitive position in the given input;
- 6 mask out the region centered at the located location in the previous step to generate an augmented sample;
- 7 set the pixel value in the selected region based on the perturbed RGB value, generating an augmented sample \mathbf{x}_i^{aug} ;
- 8 feed the augmented sample set $\{\mathbf{x}_i^{aug}, y_i\}$ to refine the network, updating the parameter w_{ind} by Equ. 4.
- 9 **return** w_{ind} as w^* ;

3.4 Fine-grained Feature Mining

To refine the network and improve its generality at most, we adopt a teacher-student pipeline to provide self-supervision. It has two advantages: on the one hand, the teacher-student pipeline can assist the network to better model the inter-class variations in facial expression recognition [48]; on the other hand, with the new coming data, the combination of cross-entropy and distillation measure can retain the knowledge from old data [49]. Unlike previous knowledge distillation methods, our work makes the teacher network and student network share the same structure. There are advantages in a few aspects: 1) in our work, the teacher network is not overparameterized, saving massive computation cost; 2) the same structure strategy saves us from the process of designing or selecting a proper teacher network.

Specifically, as illustrated in Fig. 2, in each round, the student network refined in the previous round behaves as a teacher network in the current round. The teacher network

is fixed in the current round and provides guidance to train the student network. For each sample, the trained teacher network produces a soft label for each sample, *i.e.*, the logit denoted as q_t . The logit produced by the teacher network, as well as the corresponding one-hot vector hard labels, are both utilized to supervise the training of the student network. When training the student network, the augmented samples are utilized to improve the student network generality. We use the CrossEntropy loss for the hard label, the Mean Squared Error (MSE) to minimize the discrepancy between the logit from the teacher network and the student network. The formulation is as follows:

$$\begin{aligned} \min \quad & \alpha * \text{CrossEntropy}(F_s(w_s, x_i^{\text{aug}}, y_i) \\ & + \beta * \text{MSE}(q_s(w_s, x_i^{\text{aug}}), q_t(w_t, x_i)) \end{aligned} \quad (4)$$

where $F_s(w_s, *)$ denotes the student network with parameter w_s , $q_s(w_s, x_i^{\text{aug}})$ denotes the logit generated by student network, while $q_t(w_t, x_i)$ denotes the logit generated by teacher network. α and β are parameters to balance the contribution of the two terms.

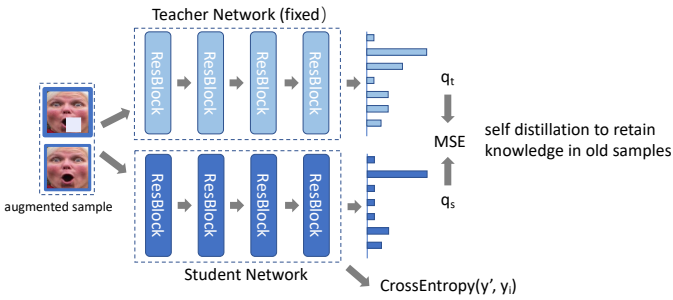


Fig. 2: The network refinement by augmented samples in a teacher-student mechanism.

Iterative Mining Mechanism. The aforementioned step can be conducted in an iterative way. In each iteration, the student network trained in the previous iteration changes its role and becomes a teacher network in the current iteration. Since the network generality is different between iterations, the located sensitive position for each image is different correspondingly. By the updated sensitive position, updated samples are feed to the student network to boost its generality in a progressive manner.

4 EXPERIMENTAL RESULTS AND DISCUSSIONS

In this section, we utilize two in-the-wild datasets, *i.e.*, FER2013 [50], Real-world Affective Face Database (RAF-DB) 2.0 [51], and one lab-controlled dataset, *i.e.*, Extended CohnKanade (CK+) [1] to demonstrate the efficacy of our method. Two kinds of evaluations are conducted, one is inner-dataset evaluation; the other one is cross-dataset evaluation. In the inner-dataset evaluation, the training set and testing set are from the same dataset; while in the cross-dataset evaluation, the training set and testing set are from different datasets. All the details about the three datasets and evaluation settings will be described in the following subsections.

4.1 Experimental Setup

We test our method on three frequently used facial expression datasets, *i.e.*, FER2013 [50], Real-world Affective Face Database (RAF-DB) 2.0 [51], Extended CohnKanade (CK+) [1]. RAF-DB and FER2013 are collected in the wild, covering variations in the real world, such as lighting conditions, large head pose, etc. To demonstrate the efficacy of our method when facing occlusion and pose issues in real scenarios, we conduct experiments on Occlusion-RAF-DB [22] and Pose-RAF-DB [22], which are constructed subsets with occlusion and pose annotations.

RAF-DB 2.0 [51] is a dataset collected from the internet. There are 29,672 facial images in this dataset. RAF-DB consists of highly diverse samples and covers different variations in the real world. The labels in this dataset are manually achieved by crowd-sourced annotation [51]. This dataset has two kinds of annotations: basic expressions and compound expressions. To make comparisons with previous works, we only utilize the basic expression label set to test our method. For the basic expression label set, there are 12,271 images for training and 3,068 images for testing.

FER2013 [50] is another widely used in-the-wild dataset. There are 28,709 samples in the training set and 3,589 samples in the testing set. All those images are collected by Google search engine and labeled with basic expressions. It was constructed for the ICML 2013 Challenges in Representation Learning. It should be noted that the original image size in this dataset is only 48×48 . The small spatial size and high variations make the analysis difficult.

CK+ [1] is a dataset collected in a lab controlled environment. The original data collected is video-based, which has 593 video sequences in total. In the first frames of each sequence, the subject activates a neutral expression and gradually shift to a peak expression to the last frames. There are 327 sequences with basic expression labels in this dataset. Unlike RAF and FER2013, there is no official training/validation/test split. Previous works usually utilize the first frame as a neutral sample and the last three frames with the target expression labels to construct the data. In the constructed data, there are 1,308 images labeled with seven basic expressions in total.

Occlusion-RAF-DB and Pose-RAF-DB [22] are occlusion test subsets extracted from RAF-DB. In those subsets, there are various occlusion types in each sample, such as masks and glasses on face, objects before faces, etc. Those constructed subsets are effective to test the efficacy of FER networks when facing real scenarios. Existing FER methods have a drop in recognition accuracy when testing in real cases full of occlusion and pose-variations [22].

Examples from those three datasets are shown in Figure. 4. There are different variations in those datasets, including: 1) scale: the spatial size of each sample in FER2013 is 48×48 , which are much smaller than that in RAF-DB and CK+; 2) lighting: the lighting conditions when capturing those datasets are quite different; 3) pose: there are heavy pose variations in RAF-DB and FER-2013, which are closer to the real testing cases.

To demonstrate the efficacy of our method, we utilize those aforementioned datasets for three evaluation settings, *i.e.*, inner-database evaluation, cross-database eval-

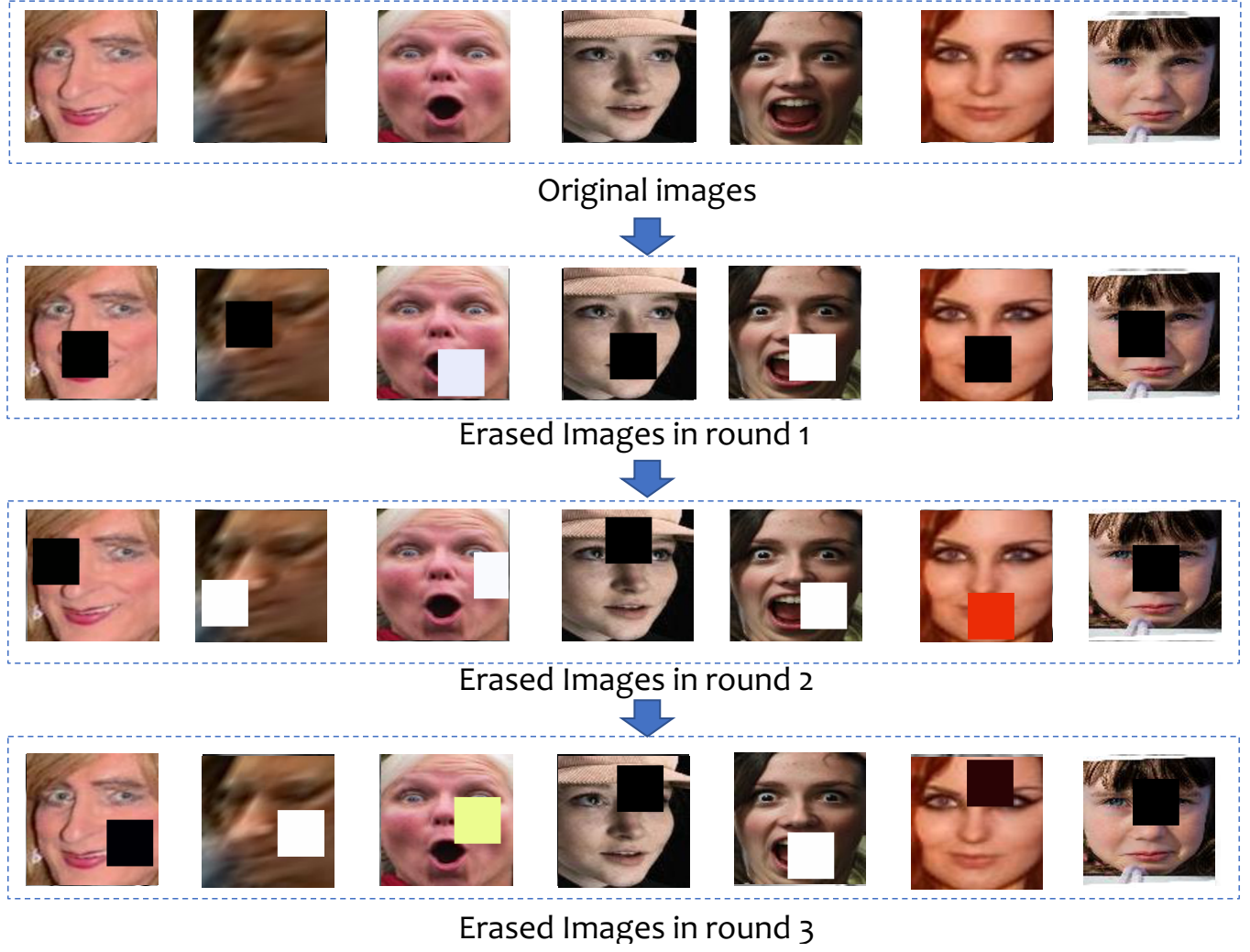


Fig. 3: Visualizing the augmented images by PASM for RAF. From top to bottom: the PASM augmented results in each round. Best viewed in color.

ation, occlusion-subset evaluation. The details of the three settings are illustrated as follows:

Inner-database Evaluation In inner-database evaluation, we train the network on the training set of a dataset and test the trained network on the testing set of the same dataset. We conduct inner-database evaluation on RAF-DB and FER2013.

Cross-database Evaluation In cross-database evaluation, we train the network on the training set of a dataset and test the trained network on a different dataset. To make a fair comparison with previous work [52], in this setting, we conduct the training on RAF-DB and test the trained network on FER2013 and CK+.

Occlusion and Pose Subset Evaluation In this setting, we train the network on RAF-DB by our method, and test it on the occlusion-raf-db and pose-raf-db, demonstrating the efficacy of our proposed method when dealing the challenging cases.

4.2 Implementation Details

In all our experiments, we detect faces and conduct the alignment based on MTCNN [53] from each given image.

All the aligned detected faces are resized to 224×224 . For making fair comparisons with previous works [52], we choose ResNet-34 and VGG16 as our backbones, which are pre-trained on ImageNet Dataset [54]. The output number for both networks are reset to seven, corresponding to the number of basic expressions. We optimize our networks by stochastic gradient descent with 0.9 momentum. We set the initial learning rate to 0.01, which will be multiplied by 0.1 when pre-specified epochs reached. We implement all the experiments in PyTorch [55] and run our experiment on NVIDIA GTX 2080Ti GPU cards.

4.3 Performance Evaluation

In this section, we test the discriminative ability of our method by conducting experiments for inner-dataset evaluations, and demonstrate the generality capability of our method by conducting experiments for cross-dataset evaluations. Our experiment is evaluated via mean classification accuracy.



Fig. 4: Visualizing the selected samples from databases utilized in this work, *i.e.*, RAF, FER2013, CK+. From left to right: neutral, anger, disgust, fear, happy, sad, and surprise. From top to bottom: RAF-DB 2.0, FER-2013, and CK+. RAF-DB 2.0 and FER-2013 are in-the-wild databases, while CK+ is a dataset collected in controlled environments. Best viewed in color.

4.3.1 Inner-dataset Evaluations

In this section, we utilize two in-the-wild databases, *i.e.*, RAF, FER2013, to demonstrate the efficacy of our method. The result comparisons on the two datasets are reported in Table.1 and 2, respectively.

Comparison on RAF We compare our method to previous state-of-the-art methods on RAF dataset and report the comparison in Table. 1. In Table. 1, [56] utilizes new loss function in their method, [57] introduces more manual labels into training and therefore needs more label cost, [58] and [22] designs region attention branch network, placing different weights on facial regions based on their occlusion conditions. Comparing to those previous works [22], [56], [57], [58], our method achieves higher performance on both chosen architectures (ResNet-34 and VGG16). Our method does not need any complex structure or any external data, but only by self mining knowledge from given data.

TABLE 1: Inner-dataset comparison of our method with previous works on RAF-DB 2.0.

Method	Year	Accuracy
baseDCNN [56]	2017	82.66
DLP-CNN [56]	2017	82.84
Center Loss [56]	2017	82.86
FSN [59]	2018	81.10
MRE-CNN [60]	2018	82.63
PAT-VGG-F-(gender,race) [57]	2018	83.83
PAT-ResNet-(gender,race) [57]	2018	84.19
OADN [58]	2020	87.16
SCN [61]	2020	87.03
RAB [22]	2020	86.90
Our method+VGG16	2020	87.50
Our method+ResNet-34 (3 round)	2020	88.68

Comparison on FER2013 We compare our method to previous state-of-the-art methods on FER2013 and report the comparison in Table. 2. FER2013 dataset was constructed for a facial expression recognition challenge. The small size of each sample and high variations introduced by pose and

light conditions make the prediction rate much lower than RAF-DB 2.0. To improve the prediction accuracy on this dataset, various methods have been proposed. For example, [57] introduced an attribute tree convolutional neural network to explicitly model the facial attributes, such as race, gender, and age. Again, our method achieves a higher performance and outperforms the previous works.

TABLE 2: Inner-dataset comparison of our method with previous works on FER-2013. The performance of previous works are cited from [62] and [36].

Method	Year	Accuracy
DLSVM. [63]	2013	71.2
Guo et al. [64]	2016	71.33
ECNN [65]	2017	69.96
Ron et al. [66]	2017	72.1
PAT-VGG-F-(gender,race). [57]	2018	72.16
PAT-ResNet-(gender,race). [57]	2018	72.00
Our method+VGG16	2020	72.73
Our method+ResNet-34 (2 round)	2020	73.59

4.3.2 Evaluations on Occlusion-RAF-DB and Pose-RAF-DB

Occlusion-RAF-DB and Pose-RAF-DB are two test subsets with manual occlusion and pose annotations. Those two datasets are constructed to test the network capability under occlusion and pose variations. [22] designed a region attention network (RAN) which adaptively assign different weights to each facial region based on their contributions. Other than that, a region biased loss is proposed to assign a higher attention weights for the regions making the most important contributions in predictions. As shown in Table. 3, our method outperformed [22] on all the sub sets. Specifically, for occlusion subset, the gain is 0.55; for pose larger than 30 degrees and 45 degrees, the gains are 2.92 and 2.97, respectively.

TABLE 3: Comparison of our method with previous works on Occlusion RAF-DB and Pose-RAF-DB.

RAF-DB	Occlusion	Pose(30)	Pose(45)
RAN [22]	82.72	86.74	85.20
Our method	83.27	89.66	88.17

4.3.3 Cross-dataset Evaluations

To test the generality of our method, we conduct a cross-dataset evaluation on three datasets. We train the network on RAF-DB and test it directly on CK+ and FER2013. The comparisons with previous works are reported in Table. 4-5. FER2013, as discussed in previous sections, is a challenging dataset collected in the real world; CK+ is collected in a lab-controlled situation and is the most representative in-the-lab dataset. We want to test the generality of our method on the lab-collected dataset and in-the-wild dataset both. Again, by self mining knowledge from given samples, our method achieves a higher cross-dataset accuracy on CK+, a comparable accuracy on FER2013.

TABLE 4: Cross-dataset comparison of our method with previous works on CK+ dataset. “6 Datasets” means MultiPIE, MMI, DISFA, FERA, SFEW, and FER2013

Method	Source	Target	Accuracy
Mollahosseini [29]	6 Datasets	CK+	64.2
Hasani et [67]	MMI+JAFFE	CK+	73.91
Wen [65]	FER-2013	CK+	76.05
Wang [68]	FER-2013	CK+	76.58
CNN-Li (VGG-F) [52]	RAF-DB2.0	CK+	78.00
Our method	RAF-DB2.0	CK+	79.65

TABLE 5: Cross-dataset comparison of our method with previous works on FER-2013 dataset. “6 Datasets” means MultiPIE, CK+, DISFA, FERA, SFEW, and FER2013

Method	Source	Target	Accuracy
Mollahosseini [29]	6 Datasets	FER-2013	34.0
CNN-Li [52]	RAF-DB2.0	FER-2013	55.38
Our method	RAF-DB2.0	FER-2013	54.78

4.4 Ablation Study

We conduct extensive ablation studies in this section to further analyze our approach. We firstly analyze the generality of the self mined knowledge; at second, we conduct a comparison with the random erasing and adversarial erasing for demonstrating the superiority of our self mined strategy; at third, we analyze the relation between the self-mining iteration number and the final accuracy; last but not the least, we illustrate the impact of the size of erasing mask and parameter in Equ. 4 to the final performance.

Generality of the Mined Adversarial Knowledge We analyze the generality of self mined knowledge extracted by our method and report the comparison in Table. 7. “Mining Network” means the sensitive regions are extracted based on PASM; the augmented samples based on the self mined knowledge are feed to “Training Network” to improve the network generality. Because [57], [58] do not have the self-mined mechanism and therefore their “Mining Network”

is left blank. To make the comparison fair, we do use the iterative refinement strategy in PASM in this experiment. On RAF-DB and FER2013, we choose ResNet-34 to mine knowledge from samples, and feed the augmented samples to a different network (VGG16). Since [57], [58] do not utilize teacher-student strategies in their works, we report our method performance without teacher-student strategy in Table. 7. This is to test the generality of the self mined knowledge from the original samples.

As shown in Table. 7, when “Training Network” is different from “Mining Network”, the prediction rate drops a bit on both of datasets. On RAF-DB, the performance drops from 87.54 to 87.09; on FER2013, the prediction rate drops from 73.50 to 72.73. We believe this performance drop comes from the difference between the characteristics of the mining network and the training network, *e.g.*, network structures, parameters. However, even when we use two different networks for self-mining and training, our performance on RAF-DB and FER2013 still outperforms or work comparably with previous works, *i.e.*, [57] and [58].

Comparison with Random Erasing and Adversarial Erasing We conduct a comparison with the random erasing [19] and adversarial erasing [20] on RAF-DB. For a fair comparison, we do not utilize knowledge distillation and iterative refinement in this experiment. The comparison results are reported in Table. 6. We can find that our method outperforms random erasing and adversarial erasing both. We suppose that the better performance of our method is from two aspects: 1) comparing to random erasing our method locates the sensitive position in each image under the adversarial attack mechanism, rather than in a purely random way; 2) comparing to adversarial erasing, our method erases the sub-region located in a more structure and sparse way, which aligns with the sparsity characteristics in face analysis problems.

TABLE 6: Comparisons with Random Erasing and Adversarial Erasing. ResNet-34 is chosen as the backbone and training for only one round. “PASM w/o teacher” denotes not using knowledge distillation strategy.

Dataset	Random Erasing	Adv Erasing	PASM w/o teacher
RAF-DB	85.93	86.57	86.86
FER2013	72.92	73.08	73.24

We show the confusion matrix comparison between PASM, Adversarial Erasing, and Random Erasing in Figure. 5. It can be observed that PASM outperforms random erasing on all expression categories, especially on “anger” (0.77 vs 0.83), “disgust” (0.59 vs 0.68).

Analysis of Self Mining Iterations In Figure. 6, we report the impact of self mining iteration numbers in our proposed method. As illustrated in Section. 3, PASM can be conducted in an iterative way. The network in the current iteration is enhanced by self mined knowledge and the corresponding augmented samples. In the following iteration, the enhanced network is utilized to further mine new knowledge from the samples, behaving as a teacher to supervise the student network training. We report the performance in each iteration on RAF and FER2013 via ResNet-34. Based on the experimental results, we can find

neutral	0.90	0.01	0.01	0.00	0.02	0.04	0.02
anger	0.04	0.83	0.05	0.02	0.02	0.01	0.02
disgust	0.11	0.06	0.68	0.01	0.05	0.09	0.01
fear	0.03	0.05	0.00	0.61	0.04	0.11	0.16
happy	0.03	0.00	0.01	0.00	0.95	0.01	0.00
sad	0.06	0.01	0.02	0.00	0.03	0.87	0.00
surprise	0.03	0.02	0.02	0.02	0.01	0.01	0.88
neutral	neutral	anger	disgust	fear	happy	sad	surprise

(a) Confusion Matrix of PASM on RAF-DB.

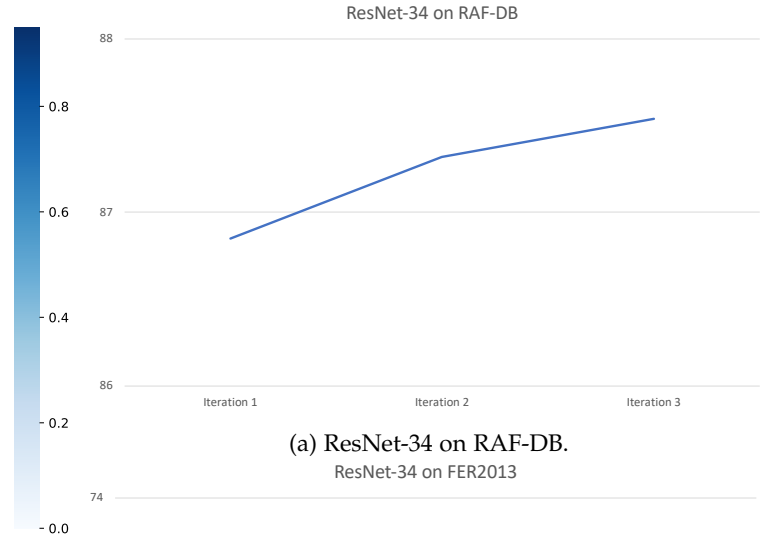
neutral	0.75	0.04	0.00	0.04	0.04	0.13	0.01
anger	0.08	0.62	0.01	0.09	0.03	0.15	0.02
disgust	0.02	0.16	0.73	0.04	0.04	0.00	0.02
fear	0.10	0.10	0.00	0.57	0.02	0.13	0.07
happy	0.03	0.01	0.00	0.01	0.91	0.02	0.02
sad	0.18	0.07	0.00	0.10	0.03	0.60	0.01
surprise	0.02	0.02	0.00	0.06	0.04	0.01	0.85
neutral	neutral	anger	disgust	fear	happy	sad	surprise

(b) Confusion Matrix of Adversarial Erasing on RAF-DB.

neutral	0.88	0.00	0.01	0.00	0.03	0.06	0.01
anger	0.05	0.77	0.06	0.01	0.06	0.01	0.03
disgust	0.14	0.06	0.59	0.01	0.08	0.09	0.03
fear	0.05	0.03	0.01	0.58	0.03	0.11	0.19
happy	0.04	0.00	0.00	0.00	0.94	0.01	0.01
sad	0.10	0.01	0.03	0.00	0.03	0.84	0.00
surprise	0.05	0.02	0.02	0.03	0.01	0.00	0.88
neutral	neutral	anger	disgust	fear	happy	sad	surprise

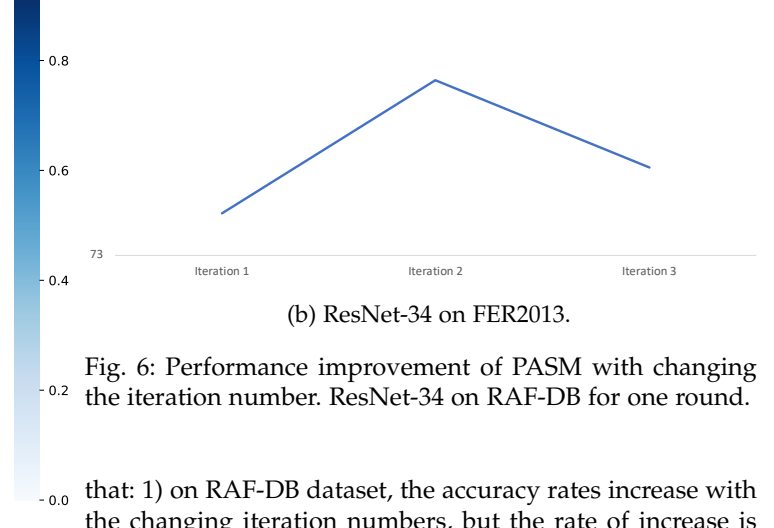
(c) Confusion Matrix of Random Erasing on RAF-DB.

Fig. 5: Confusion Matrix Comparison between Random Erasing and PASM on RAF-DB by ResNet-34. The darker the color, the higher the accuracy.



(a) ResNet-34 on RAF-DB.

ResNet-34 on FER2013



(b) ResNet-34 on FER2013.

Fig. 6: Performance improvement of PASM with changing the iteration number. ResNet-34 on RAF-DB for one round.

that: 1) on RAF-DB dataset, the accuracy rates increase with the changing iteration numbers, but the rate of increase is decreasing; 2) on FER2013, the accuracy rates increase first, after two iteration refinements, the performance starts to drop.

Analysis of Mask Sizes and Parameter Configuration in Equ. 4 In Fig. 7, we report the prediction accuracy with different mask sizes, which is trained on RAF-DB by a ResNet-34 for one round. We choose five different mask sizes, *i.e.*, from 23 to 39 with a step size of 4. In the figure, we can find that the accuracy is not very sensitive to the mask sizes since the accuracy differences between various mask sizes are little.

In Fig. 8, we show the prediction accuracy with parameter configuration in Equ. 4. In this experiment, we also trained on RAF-DB via a ResNet-34 for one round. We choose the α as 1 and change β to 0.5, 0.1, 0.01 respectively. In the figure, we can find that the accuracy is stable with those different parameter configuration.

Shortage and Limitation of PASM Although PASM is able to self mine knowledge from given data by analyzing the statistical information of data and network parameters, there are a few limitations of this method: 1) the sensitive position search is time-consuming. The key computation ingredient in our method is based on point adversarial attack, which is time-consuming and therefore limit its applicability

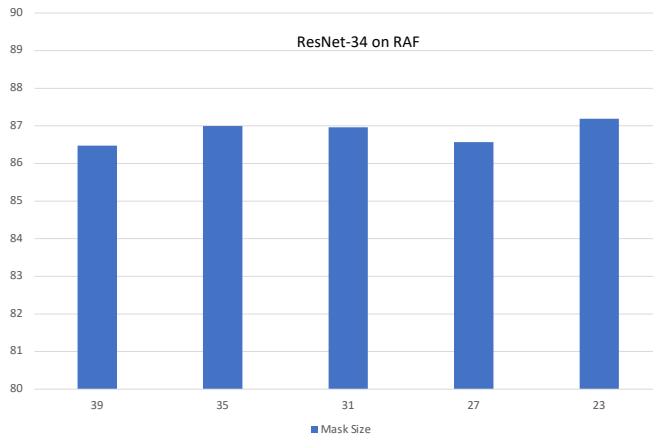


Fig. 7: Evaluation with different mask sizes for final accuracy. ResNet-34 trained on RAF-DB.

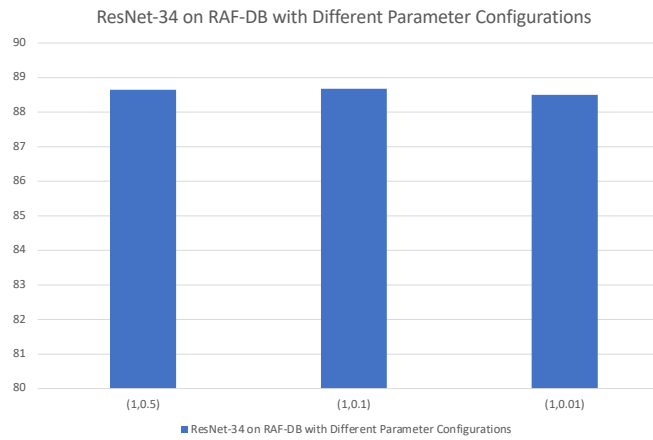


Fig. 8: Evaluation with different parameter configuration in Equ. 4 for final accuracy. ResNet-34 trained on RAF-DB.

on the dataset with huge sizes. To solve this problem, a real time adversarial attack method becomes necessary. 2) an automatic and adaptive way for choosing an appropriate iteration number in PASM is expected. Current now, it is still needed to be set manually. We leave those two aspects to our future work.

TABLE 7: Study of Self Mined Information Generality

Dataset	Mining Network	Training Network	Accuracy
PAT [57]	-	ResNet-34	83.83
PAT [57]	-	VGG-16	84.19
OADN [58]	-	ResNet-50	87.16
PASM	ResNet-34	ResNet-34	87.54
PASM	ResNet-34	VGG-16	87.09
PAT [57]	-	ResNet-34	72.16
PAT [57]	-	VGG-16	72.00
PASM	ResNet-34	ResNet-34	73.50
PASM	ResNet-34	VGG-16	72.73

5 CONCLUSION

In this article, we propose a self mining framework based on point adversarial attack and name it as Point Adversarial Self Mining (PASM). PASM does not need to utilize

complex networks designed manually and/or sophisticated loss functions for high accuracy. On the contrary, it manages to self mine knowledge from given samples by considering the model-specified contribution for different regions to the classification in each sample. Other than that, PASM can be conducted in an iterative way, keeping to enhance the performance progressively. In our experiment results, we have observed that the PASM achieves significant advancement for facial expression recognition in the wild.

REFERENCES

- [1] P. Lucey, J. F. Cohn, T. Kanade, J. Saragih, Z. Ambadar, and I. Matthews, "The extended cohn-kanade dataset (ck+): A complete dataset for action unit and emotion-specified expression," in *CVPR-W*, 2010.
- [2] Z. Zhang, M. Lyons, M. Schuster, and S. Akamatsu, "Comparison between geometry-based and gabor-wavelets-based facial expression recognition using multi-layer perceptron," in *FG*, 1998.
- [3] Y. Zhang and Q. Ji, "Active and dynamic information fusion for facial expression understanding from image sequences," *IEEE Transactions on Pattern Analysis and Machine Intelligence*, 2005.
- [4] Y.-l. Tian, T. Kanade, and J. F. Cohn, "Evaluation of gabor-wavelet-based facial action unit recognition in image sequences of increasing complexity," in *FG*, 2002.
- [5] M. Eckhardt, I. Fasel, and J. Movellan, "Towards practical facial feature detection," *IJPRAI*, 2009.
- [6] P. Yang, Q. Liu, and D. N. Metaxas, "Boosting coded dynamic features for facial action units and facial expression recognition," in *CVPR*, 2007.
- [7] Y. Hu, Z. Zeng, L. Yin, X. Wei, X. Zhou, and T. S. Huang, "Multi-view facial expression recognition," in *FG*, 2008.
- [8] M. Dahmane and J. Meunier, "Emotion recognition using dynamic grid-based hog features," in *FG*, 2011.
- [9] S. Han, Z. Meng, P. Liu, and Y. Tong, "Facial grid transformation: A novel face registration approach for improving facial action unit recognition," in *ICIP*, 2014.
- [10] P. Liu, S. Han, Z. Meng, and Y. Tong, "Facial expression recognition via a boosted deep belief network," in *CVPR*, 2014.
- [11] Z. Meng, P. Liu, J. Cai, S. Han, and Y. Tong, "Identity-aware convolutional neural network for facial expression recognition," in *FG*, 2017.
- [12] J. Su, D. V. Vargas, and K. Sakurai, "One Pixel Attack for Fooling Deep Neural Networks," *IEEE Transactions on Evolutionary Computation*, 2019.
- [13] G. Hinton, O. Vinyals, and J. Dean, "Distilling the knowledge in a neural network," in *NeurIPS Workshop*, 2015.
- [14] H. Zhang, W. Su, and Z. Wang, "Weakly Supervised Local-Global Attention Network for Facial Expression Recognition," in *IJCAI*, 2020.
- [15] Y. Li, J. Zeng, S. Shan, and X. Chen, "Occlusion aware facial expression recognition using cnn with attention mechanism," *IEEE Transactions on Image Processing*, 2019.
- [16] Y. Liu, J. Peng, J. Zeng, and S. Shan, "Pose-adaptive Hierarchical Attention Network for Facial Expression Recognition," *arxiv*, 2019. [Online]. Available: <http://arxiv.org/abs/1905.10059>
- [17] K. He, X. Zhang, S. Ren, and J. Sun, "Deep residual learning for image recognition," in *CVPR*, 2016.
- [18] K. Simonyan and A. Zisserman, "Very deep convolutional networks for large-scale image recognition," in *ICLR*, 2015.
- [19] Z. Zhong, L. Zheng, G. Kang, S. Li, and Y. Yang, "Random erasing data augmentation arxiv 2017," in *AAAI*, 2020.
- [20] Y. Wei, J. Feng, X. Liang, M.-M. Cheng, Y. Zhao, and S. Yan, "Object region mining with adversarial erasing: A simple classification to semantic segmentation approach," in *CVPR*, 2017.
- [21] L. Zhong, Q. Liu, P. Yang, B. Liu, J. Huang, and D. N. Metaxas, "Learning active facial patches for expression analysis," in *CVPR*, 2012.
- [22] K. Wang, X. Peng, J. Yang, D. Meng, and Y. Qiao, "Region Attention Networks for Pose and Occlusion Robust Facial Expression Recognition," *IEEE Transactions on Image Processing*, 2020.
- [23] Z. Zeng, M. Pantic, G. I. Roisman, and T. S. Huang, "A survey of affect recognition methods: Audio, visual, and spontaneous expressions," *IEEE Transactions on Pattern Analysis and Machine Intelligence*, 2008.

[24] E. Sariyanidi, H. Gunes, and A. Cavallaro, "Automatic analysis of facial affect: A survey of registration, representation, and recognition," *IEEE Transactions on Pattern Analysis and Machine Intelligence*, 2014.

[25] T. Zhang, "Facial expression recognition based on deep learning: a survey," in *International Conference on Intelligent and Interactive Systems and Applications*, 2017.

[26] T. Senechal, V. Rapp, H. Salam, R. Seguier, K. Bailly, and L. Prevost, "Combining aam coefficients with lgbp histograms in the multi-kernel svm framework to detect facial action units," in *FG*, 2011.

[27] M. F. Valstar, M. Mehu, B. Jiang, M. Pantic, and K. Scherer, "Meta-analysis of the first facial expression recognition challenge," *IEEE Transactions on Systems, Man, and Cybernetics, Part B (Cybernetics)*, 2012.

[28] P. Liu, J. T. Zhou, I. W.-H. Tsang, Z. Meng, S. Han, and Y. Tong, "Feature disentangling machine-a novel approach of feature selection and disentangling in facial expression analysis," in *ECCV*, 2014.

[29] A. Mollahosseini, D. Chan, and M. H. Mahoor, "Going deeper in facial expression recognition using deep neural networks," in *WACV*, 2016.

[30] F. Zhang, T. Zhang, Q. Mao, and C. Xu, "Joint pose and expression modeling for facial expression recognition," in *CVPR*, 2018.

[31] H. Yang, U. Ciftci, and L. Yin, "Facial expression recognition by de-expression residue learning," in *CVPR*, 2018.

[32] B. Hu, Z. Zheng, P. Liu, W. Yang, and M. Ren, "Unsupervised eyeglasses removal in the wild," *IEEE Transactions on Cybernetics*, 2020.

[33] Y. Zhang, I. W. Tsang, J. Li, P. Liu, X. Lu, and X. Yu, "Face hallucination with finishing touches," *arXiv preprint arXiv:2002.03308*, 2020.

[34] Z. Meng, S. Han, P. Liu, and Y. Tong, "Improving speech related facial action unit recognition by audiovisual information fusion," *IEEE Transactions on Cybernetics*, 2019.

[35] J. Cai, Z. Meng, A. S. Khan, Z. Li, J. O'Reilly, S. Han, P. Liu, M. Chen, and Y. Tong, "Feature-level and model-level audiovisual fusion for emotion recognition in the wild," in *MIPR*, 2019.

[36] L. Shan and D. Weihong, "Deep Facial expression recognition: A survey," *IEEE Transactions on Affective Computing*, 2020.

[37] A. Krizhevsky, I. Sutskever, and G. E. Hinton, "Imagenet classification with deep convolutional neural networks," in *NeurIPS*, 2012.

[38] H. Zhang, M. Cissé, Y. N. Dauphin, and D. Lopez-Paz, "mixup: Beyond empirical risk minimization," in *ICLR*, 2018.

[39] C. Shorten and T. M. Khoshgoftaar, "A survey on image data augmentation for deep learning," *Journal of Big Data*, 2019.

[40] C. Szegedy, W. Zaremba, I. Sutskever, J. Bruna, D. Erhan, I. Goodfellow, and R. Fergus, "Intriguing properties of neural networks. arxiv 2013," *arXiv preprint arXiv:1312.6199*, 2013.

[41] S. Rao, D. Stutz, and B. Schiele, "Adversarial Training against Location-Optimized Adversarial Patches," *arxiv*, 2020.

[42] I. J. Goodfellow, J. Shlens, and C. Szegedy, "Explaining and harnessing adversarial examples," *arXiv preprint arXiv:1412.6572*, 2014.

[43] S.-M. Moosavi-Dezfooli, A. Fawzi, and P. Frossard, "Deepfool: a simple and accurate method to fool deep neural networks," in *CVPR*, 2016.

[44] A. Kurakin, I. Goodfellow, and S. Bengio, "Adversarial machine learning at scale," *arXiv preprint arXiv:1611.01236*, 2016.

[45] L. Jiang, X. Ma, S. Chen, J. Bailey, and Y.-G. Jiang, "Black-box adversarial attacks on video recognition models," in *MM*, 2019.

[46] N. Papernot, P. McDaniel, I. Goodfellow, S. Jha, Z. B. Celik, and A. Swami, "Practical black-box attacks against machine learning," in *ASIA CCS 2017 - Proceedings of the 2017 ACM Asia Conference on Computer and Communications Security*, 2017.

[47] O. Russakovsky, J. Deng, H. Su, J. Krause, S. Satheesh, S. Ma, Z. Huang, A. Karpathy, A. Khosla, M. Bernstein, A. C. Berg, and L. Fei-Fei, "ImageNet Large Scale Visual Recognition Challenge," *International Journal of Computer Vision (IJCV)*, 2015.

[48] Z. Zheng, X. Yang, Z. Yu, L. Zheng, Y. Yang, and J. Kautz, "Joint discriminative and generative learning for person re-identification," in *CVPR*, 2019.

[49] F. M. Castro, M. J. Marín-Jiménez, N. Guil, C. Schmid, and K. Alahari, "End-to-end incremental learning," in *ECCV*, 2018.

[50] I. J. Goodfellow, D. Erhan, P. L. Carrier, A. Courville, M. Mirza, B. Hamner, W. Cukierski, Y. Tang, D. Thaler, D.-H. Lee *et al.*,

"Challenges in representation learning: A report on three machine learning contests," *Neural Networks*, 2015.

[51] S. Li and W. Deng, "Reliable crowdsourcing and deep locality-preserving learning for unconstrained facial expression recognition," *IEEE Transactions on Image Processing*, 2018.

[52] —, "A Deeper Look at Facial Expression Dataset Bias," *IEEE Transactions on Affective Computing*, 2020.

[53] K. Zhang, Z. Zhang, Z. Li, and Y. Qiao, "Joint face detection and alignment using multitask cascaded convolutional networks," *IEEE Signal Processing Letters*, 2016.

[54] J. Deng, W. Dong, R. Socher, L.-J. Li, K. Li, and L. Fei-Fei, "Imagenet: A large-scale hierarchical image database," in *CVPR*, 2009.

[55] A. Paszke, S. Gross, F. Massa, A. Lerer, J. Bradbury, G. Chanan, T. Killeen, Z. Lin, N. Gimelshein, L. Antiga, A. Desmaison, A. Kopf, E. Yang, Z. DeVito, M. Raison, A. Tejani, S. Chilamkurthy, B. Steiner, L. Fang, J. Bai, and S. Chintala, "Pytorch: An imperative style, high-performance deep learning library," in *NeurIPS*, 2019.

[56] S. Li, W. Deng, and J. Du, "Reliable crowdsourcing and deep locality-preserving learning for expression recognition in the wild," in *CVPR*, 2017.

[57] J. Cai, Z. Meng, A. S. Khan, Z. Li, J. O'Reilly, and Y. Tong, "Probabilistic attribute tree in convolutional neural networks for facial expression recognition," *arXiv preprint arXiv:1812.07067*, 2018.

[58] H. Ding, P. Zhou, and R. Chellappa, "Occlusion-adaptive deep network for robust facial expression recognition," *arXiv preprint arXiv:2005.06040*, 2020.

[59] S. Zhao, H. Cai, H. Liu, J. Zhang, and S. Chen, "Feature selection mechanism in cnns for facial expression recognition," in *BMVC*, 2018.

[60] Y. Fan, J. C. Lam, and V. O. Li, "Multi-region ensemble convolutional neural network for facial expression recognition," in *ICANN*, 2018.

[61] K. Wang, X. Peng, J. Yang, S. Lu, and Y. Qiao, "Suppressing uncertainties for large-scale facial expression recognition," in *CVPR*, 2020.

[62] J. Cai, "Improving person-independent facial expression recognition using deep learning," 2019.

[63] Y. Tang, "Deep learning using linear support vector machines," *arXiv preprint arXiv:1306.0239*, 2013.

[64] Y. Guo, D. Tao, J. Yu, H. Xiong, Y. Li, and D. Tao, "Deep neural networks with relativity learning for facial expression recognition," in *ICMEW*, 2016.

[65] G. Wen, Z. Hou, H. Li, D. Li, L. Jiang, and E. Xun, "Ensemble of deep neural networks with probability-based fusion for facial expression recognition," *Cognitive Computation*, 2017.

[66] R. Breuer and R. Kimmel, "A deep learning perspective on the origin of facial expressions," *arXiv preprint arXiv:1705.01842*, 2017.

[67] B. Hasani and M. H. Mahoor, "Spatio-temporal facial expression recognition using convolutional neural networks and conditional random fields," in *FG*, 2017.

[68] X. Wang, X. Wang, and Y. Ni, "Unsupervised domain adaptation for facial expression recognition using generative adversarial networks," 2018.